

# The cognitive control network: Integrated cortical regions with dissociable functions

Michael W. Cole<sup>a,b,\*</sup> and Walter Schneider<sup>a,c</sup>

<sup>a</sup>Center for the Neural Basis of Cognition, Center for Neuroscience, and Learning Research and Development Center, University of Pittsburgh, PA 15260, USA

<sup>b</sup>Department of Neuroscience, University of Pittsburgh, PA 15260, USA

<sup>c</sup>Department of Psychology, University of Pittsburgh, PA 15260, USA

Received 12 September 2006; revised 26 March 2007; accepted 29 March 2007

Available online 25 April 2007

Consensus across hundreds of published studies indicates that the same cortical regions are involved in many forms of cognitive control. Using functional magnetic resonance imaging (fMRI), we found that these coactive regions form a functionally connected cognitive control network (CCN). Network status was identified by convergent methods, including: high inter-regional correlations during rest and task performance, consistently higher correlations within the CCN than the rest of cortex, co-activation in a visual search task, and mutual sensitivity to decision difficulty. Regions within the CCN include anterior cingulate cortex/pre-supplementary motor area (ACC/pSMA), dorsolateral prefrontal cortex (DLPFC), inferior frontal junction (IFJ), anterior insular cortex (AIC), dorsal pre-motor cortex (dPMC), and posterior parietal cortex (PPC). We used a novel visual line search task which included periods when the probe stimuli were occluded but subjects had to maintain and update working memory in preparation for the sudden appearance of a probe stimulus. The six CCN regions operated as a tightly coupled network during the ‘non-occluded’ portions of this task, with all regions responding to probe events. In contrast, the network was differentiated during occluded search. DLPFC, not ACC/pSMA, was involved in target memory maintenance when probes were absent, while both regions became active in preparation for difficult probes at the end of each occluded period. This approach illustrates one way in which a neuronal network can be identified, its high functional connectivity established, and its components dissociated in order to better understand the interactive and specialized internal mechanisms of that network.

© 2007 Elsevier Inc. All rights reserved.

## Introduction

An act as common as searching for a friend in a crowd can involve many cognitive control processes. Such processes include, among others, target working memory (keeping in mind what your friend looks like), attention to stimuli (viewing the individuals in

the crowd), target–stimulus comparison (deciding if the viewed individual is your friend), response preparation (determining what to do if you see your friend), and response initiation (initiating the planned motor response to get your friend’s attention). These same components are involved in a large variety of tasks, both in daily life and in the cognitive control neuroimaging literature. This is the case because any novel or conflict-laden task requires a set of instructions/intentions to be dynamically converted to stimulus–response (S–R) associations for proper task performance. As illustrated above, this conversion can involve a number of processes.

A collection of neural components of similar number to the above collection of cognitive components is consistently involved in a large variety of cognitive control tasks as well (see Cabeza and Nyberg, 2000; Duncan and Owen, 2000; Schneider and Chein, 2003; Wager et al., 2004; Brass et al., 2005; Chein and Schneider, 2005; Dosenbach et al., 2006). These neural components include dorsolateral prefrontal cortex (DLPFC), anterior cingulate cortex/pre-supplementary motor area (ACC/pSMA), dorsal premotor cortex (dPMC), anterior insular cortex (AIC), inferior frontal junction (IFJ), and posterior parietal cortex (PPC). The present study examines the proposal that this set of regions forms a cognitive control network (CCN) of anatomically distinct component processing brain regions that interact in a tightly coupled fashion to implement cognitive control in a variety of task contexts.

The trouble with tightly coupled networks is that their components can be difficult to clearly dissociate, and the CCN is no exception. As mentioned above, most cognitive control tasks involve the same set of component processes. Additionally, most of these processes have to occur in the short temporal window between stimulus and response (~500 ms typically). This makes it difficult to separate task processes with a technique such as functional magnetic resonance imaging (fMRI) which has a multi-second response function. Also, many of these processes (e.g., working memory and target–stimulus comparison) must interact in order for information from one process to influence the other. The highly interactive nature of these processes makes component separation problematic, though factorial analysis (e.g., showing

---

\* Corresponding author. 3939 O’Hara Street, 631 LRDC, Pittsburgh, PA 15260, USA.

E-mail address: mwc4@pitt.edu (M.W. Cole).

Available online on ScienceDirect ([www.sciencedirect.com](http://www.sciencedirect.com)).

one region has greater sensitivity to difficulty relative to another) can be used to separate these components in some cases.

The present study employed an alternative approach in which the S–R processes were separated from the initiation, maintenance, and preparation of the CCN for task performance. This allowed working memory initiation and maintenance to be observed separately from response preparation, and all three processes to be observed separately from the many components of S–R processing. A mixed blocked/event-related task design, which can be used to separate estimates of sustained from transient neural processes (Visscher et al., 2003), was used to accomplish these component separations.

Duncan and Owen (2000) pointed out that two of the regions mentioned above, DLPFC and ACC/pSMA, have especially highly correlated activation patterns across a large variety of task demands across a large number of studies. There are very few claims of having separated these regions despite the many studies reporting activity in them. MacDonald et al. (2000) have made one of the strongest claims to this effect. They found that cues indicating hard vs. cues indicating easy upcoming probes showed a larger response in DLPFC (not ACC/pSMA), while comparing hard vs. easy probes showed a larger response in ACC/pSMA (not DLPFC). This result has not been supported by several recent studies looking at preparatory cues (see Luks et al., 2002; Brown and Braver, 2005; Luks et al., 2007; Schumacher et al., 2007). For instance, Schumacher et al. (2007) found that DLPFC activity was increased by both cue and probe difficulty.

A number of studies have shown that DLPFC responds to working memory demands while ACC/pSMA does not (e.g., Barch et al., 1997; Manoach et al., 1997; Smith et al., 1998; Ranganath and D'Esposito, 2001). This is perhaps the most consistently characterized difference between the two regions, and yet there are a number of studies that have shown ACC/pSMA activity during working memory delays (see Wager and Smith, 2003 for review). For instance, Petit et al. (1998) showed sustained activity within ACC/pSMA during both spatial and face working memory maintenance.

We hypothesized that ACC/pSMA is involved during working memory delays due to its involvement in preparatory processes, while DLPFC is involved during working memory delays due to active maintenance of task goal information. We hypothesized that both regions are involved in S–R processing.

In order to test these hypotheses, we used a modified visual search task, the occluded target switching paradigm, to separate target maintenance and preparatory activity from S–R processing activity. The basic task involved presentation of a line orientation every second with the goal being to press a button whenever the target orientation appeared. In this modified task, target maintenance was separated from probe processing using ‘occluded’ periods in which very few probes occurred and the main task demand was to actively maintain the present target in memory (“non-switch trials”; see Fig. 1A). In another occluded condition, targets were switched internally (i.e., working memory was updated) every 4 s between two highly familiar line orientations (i.e., “/” and “\”), such that the main task demand was not only to maintain the current target but also to update the current target periodically (“target switch trials”; see Fig. 1B).

We expected DLPFC, not ACC/pSMA, to be active throughout both of these occluded periods. We expected ACC/pSMA to be active as well during the final third of the target switching occluded period, since subjects were much more likely to prepare for an upcoming probe during this time. Preparation was more likely toward the end of the occluded period because there was a much higher probability of a probe at the end relative to the rest of each occluded period (~10× increased chance; learned through practice with the task). We expected that less preparation-related activity would be present during the non-switching condition since S–R mappings remained consistent throughout each of these trials, while in the target switching condition S–R mappings were variable, causing an increased need for control (Schneider and Shiffrin, 1977) and thus increasing the need for preparation for these more demanding probes.

DLPFC and ACC/pSMA are not the only regions that are coactive across a large variety of cognitive control task demands. As mentioned above, a consensus has emerged that a set of six regions (DLPFC, ACC/pSMA, dPMC, IFJ, AIC, and PPC) is involved in core cognitive control functions. We hypothesized that this set of cognitive control regions forms a functionally connected network for implementing cognitive control.

In accordance with the functional integration of these regions, as well as its proposed role in cognitive control, we predicted that the entire network would be active during S–R processing and many/all areas of the network would show sensitivity to S–R

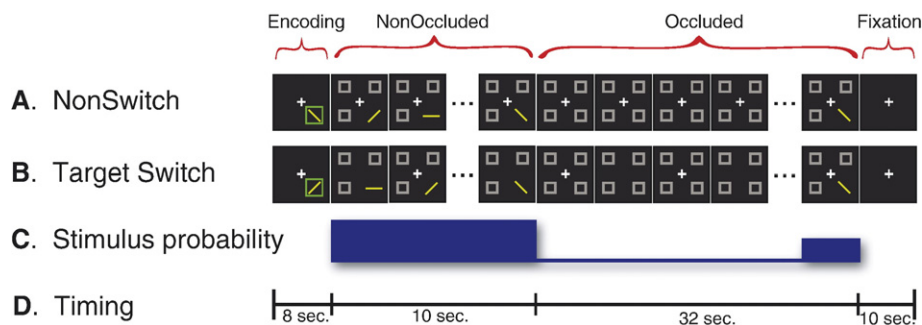


Fig. 1. The occluded line search task. Each of two trial types consisted of four periods in the following order: Encoding (8 s), NonOccluded (10 s), Occluded (32 s), and Fixation (10 s). Each line orientation probe lasted one second. (A) During NonSwitch trials subjects maintained the same target in the same location. (B) During Target Switch trials the target line orientation was switched every four seconds (indicated by a brief removal of the fixation cross). The second target was also presented simultaneously during encoding, though this is not depicted in the diagram. (C) The probability of a stimulus appearing varied from 100% during the NonOccluded period, to 5% during the majority of the Occluded period, and 55% at the end of the Occluded period. (D) Timing information across the trial periods, with each trial lasting exactly 1 min.

processing difficulty. We used a varied mapping manipulation (see Schneider and Shiffrin, 1977) in which subjects searched for either a 45° or 135° oriented line (i.e., “/” or “\”) among serially presented probes consisting of 0°, 90°, 45°, or 135° (i.e., “—”, “|”, “/”, or “\”). There were three types of probe S–R mappings: distracters, targets, and foils. Pure distracters were probes (0° or 90°) that never required a response and were consistently irrelevant to the task throughout the experiment. Distracters required very little cognitive control since once recognized they could be easily ignored. Target and foil probes were selected from a common pool of line stimuli. Therefore, the current foil probe was previously a target and vice versa. To illustrate: assume in trial 1 the subject searched for “\” and on trial 2 for “/”. On trial 2 the appearance of “—” would be a distracter, “/” would be the target, and “\” the foil. Trial 1 had built up the association that “\” was the target, but on trial two this association was not only irrelevant but also conflicting with the correct S–R process.

The conflict engendered by this S–R inconsistency manipulation was of the most demanding type (negative priming; see Malley and Strayer, 1995). We hypothesized that the entire set of regions, the CCN, would respond to these high conflict situations because they are the most demanding for cognitive control processes. This finding would support the central role of these regions in cognitive control, and it would also support their hypothesized functional unity.

Inter-regional functional connectivity was assessed in order to firmly establish the functional unity of the CCN. The proposal that the CCN is a highly integrated functional network predicts (1) that the network has high internal functional connectivity. Further, it predicts (2) that this internal functional connectivity is higher than CCN connectivity to non-CCN regions, and also (3) higher than average connectivity between all cortical regions. An additional prediction inherent in the proposed role of this network (i.e., monitoring and controlling much of cortex) is (4) that CCN connectivity to non-CCN regions is higher than the average connectivity between all cortical regions.

Resting state correlations in fMRI signals were used to assess functional connectivity in order to rule out connectivity patterns tied to any specific task. The fluctuations underlying these correlations likely originate from spontaneous slow-wave electrical activity across cortex. Golanov et al. (1994) showed that such spontaneous electrical activity occurs across cortex in anaesthetized rats, and is followed by increases in regional cerebral blood flow lasting ~12 s. Such increases in blood flow are known to increase the blood oxygen level dependent (BOLD) signal, as measured by fMRI (Ogawa et al., 1992). Furthermore, Golanov et al. found that these spontaneous waves of electrical activity and the corresponding blood flow changes ( $R=0.94$  between these events) occurred at ~0.1 Hz, which is approximately the same rate as resting state BOLD fluctuations in humans (Cordes et al., 2001). These slow BOLD fluctuations are correlated between functionally connected regions (Xiong et al., 1999) likely because when two regions are anatomically connected with significant synaptic weights these connections do not “turn off” when not being used for task performance. Instead, any spontaneous neural firing in one region will likely cause an increase in action potential propagation across even long-distance axonal connections. Thus, once potential confounding signals are dealt with (see Materials and methods), resting state BOLD correlations likely reflect functional connectivity as utilized by task performance. Supporting this conclusion, Cordes et al. (2000) found very similar patterns across cortex when comparing fMRI

functional activity (using motor, language, and visual tasks) and cortex-wide resting state correlations. BOLD correlations between well-known functionally and anatomically connected regions (e.g., LIP and FEF) have been found in anaesthetized monkeys as well (Vincent et al., 2007).

## Materials and methods

### Subjects

We included nine right-handed subjects (7 male, 2 female), aged 19 to 42 in the study. These subjects were recruited from the University of Pittsburgh and surrounding area. Subjects were excluded if they had any medical, neurological, or psychiatric illness, any contraindications for MRI scans, or were left-handed. All subjects gave informed consent.

### Cognitive task

The basic task was to detect a target line orientation by comparing it to each serially presented stimulus (see Fig. 1). The target could be one of two possible line orientations: 45° (“/”) or 135° (“\”). Subjects pressed a button with their right index finger when the target was present, and refrained from button pressing if the target was not present. E-Prime (Psychology Software Tools, Inc., Pittsburgh, PA; see Schneider et al., 2002) was used on a Windows PC for task presentation and response collection.

Seven of the subjects performed 12 five-minute runs, while the other two performed 10 and 11 runs, respectively, due to time constraints. Each run consisted of five, one-minute trials, each of a different type. The five trial conditions included: target switching, location switching, non-switching with a blinking fixation stimulus (blink non-switching), non-switching without a blinking fixation stimulus (non-blink non-switching), and resting fixation. These trials occurred in random order within each run, with the constraint that the resting fixation trial occur only in one of the middle three slots to ensure that any linear trend removal of the data was not skewed by a low-activity condition occurring on either end of a given run.

Each trial began with 8 s of encoding (task instructions, including target encoding), followed by 10 s of stimuli presented once every second (non-occluded period). The next 32 s consisted of an occluded period in which subjects maintained the task context and were infrequently presented with probes. Fifty percent of the trials (uncued, ordered randomly) presented only one probe at the end of the occluded period; the other 50% of trials had a low probability (5%) of having a probe within any one second interval, and typically had one to two probes per trial. This meant that there was a much higher probability of probes occurring in the final portion of the occluded period than at any other time (see Fig. 1C). Finally, each trial ended with 10 s of resting fixation.

In the target switching condition subjects switched between a 45° target and a 135° target whenever the central fixation disappeared briefly (one second). This fixation blink occurred every 4 s, beginning just after encoding and continuing throughout the non-occluded and occluded periods. Each trial began with encoding of one of the two possible target line orientations, each occurring randomly with equal probability. Additionally, the location of the stimuli was indicated (one of four potential locations, randomly selected) and the second target stimulus was

placed in the lower right corner of the screen (outside the stimulus presentation area to serve as a reminder) for the duration of the encoding period.

The fixation blink occurred at the same rate during the location switching condition, but signaled a location switch rather than a target switch. Subjects switched the attended location while performing target search. Results from the location switching condition are not reported here.

The non-switching conditions were identical to the switching conditions except that only one target orientation was utilized during a trial. For each trial, the target was randomly selected from 45° and 135°, with a higher probability of 45° (75%) than 135° (25%). In the non-blink non-switching condition, the fixation was stable throughout the trial, whereas in the blink non-switching condition the fixation blinked every 4 s just like in the switching condition. However, the instructions at the beginning indicated to the participants that this was a non-switching condition and therefore the blink was irrelevant. The blink non-switch was perhaps a better control for the switching conditions because it equated the visual aspects of the task better. However, the non-blink condition was included in case the data showed large, unexpected effects due to the irrelevant blink. Analysis revealed no significant increases for the blink vs. non-blink conditions (voxel-wise  $P < 0.05$ , false discovery rate (FDR) corrected for multiple comparisons), so they were considered identical and were combined as a single condition in the final analysis.

Finally, the resting fixation trials consisted of an 8 s instruction screen (indicating a rest period had begun) followed by 52 s of a stable white fixation cross on a black background.

#### *MRI data collection*

Image acquisition was carried out on a 3T Siemens Allegra MRI scanner. Thirty-four transaxial slices were acquired every 2 s (FOV: 210, TE: 30, Flip angle: 70, Slice thickness: 3 mm), with a total of 150 EPI volumes collected per run. Three-dimensional anatomical MP-RAGE images and T2 structural in-plane images were collected for each subject.

#### *MRI data analysis*

BrainVoyager QX (Brain Innovation; Maastricht, The Netherlands) was used to perform pre-processing and general linear model (GLM) analyses. The Talairach Daemon software tool was used for determining anatomical labels for foci of interest (Lancaster et al., 2000). Matlab (The MathWorks; Natick, MA) was used to perform functional connectivity analyses and ROI-based analysis of variance (ANOVA) procedures. All ANOVAs were non-repeated measures and used subjects as a random effect (all other factors were fixed effects). Only correct probes were used for the probe analyses.

All functional images were realigned to the first image of each run, which were aligned to the first run of each subject. Signal for each voxel was spatially smoothed across 8 mm, FWHM. Each subject's in-plane anatomical images were co-registered to their MP-RAGE and this transformation was applied to the functional images. These images were then transformed into a canonical Talairach space (Talairach and Tournoux, 1988). GLM, time series, and connectivity analyses are reported here as grouped data encompassing data from the nine subjects.

The GLM analysis for the encoding, non-occluded, occluded, and resting fixation periods were performed using boxcars sustained over the duration of each condition and convolved with a hemodynamic response function. Transient, probe-related effects were modeled using separate regressors for each time point (deconvolution analysis). This approach was very similar to that used for the mixed block/event-related designs reported elsewhere (e.g., Visscher et al., 2003; Dosenbach et al., 2006). Visscher et al. showed that sustained and transient signals can be separated using GLM analysis, especially when using multiple regressors for transient events as was done here. The present study employed long blank (occluded) periods in order to further ensure that no transient signals contaminated the sustained regressors. Rather than being modeled by one long sustained regressor each occluded period was separated into thirds of equal duration, with separate convolved boxcars (the sustained regressors) over each third.

Voxel-wise contrasts were conducted using BrainVoyager QX. Each statistical contrast was between regressors used in the GLM analysis, which was performed across all voxels independently. The conjunction of multiple contrasts used in several cases in the present study (both for voxel-wise and ROI GLMs) provides a logical AND between the contrasts, such that all statistically significant voxels in the conjunction of contrast A and contrast B are also statistically significant for each contrast independently.  $T$ -values reported with the conjunction analyses are based on a 'conjunction null distribution' derived from all contrasts used in the conjunction (see Nichols et al., 2005). Unless noted otherwise, all contrasts used a false discovery rate (FDR) correction for multiple comparisons (see Genovesi et al., 2002).

Regions of interest (ROIs) were defined by the regions active ( $P < 0.05$ , FDR corrected) during the non-occluded target switching period vs. the non-occluded non-switching period (see Fig. 2 and Table 1). These same ROIs were used for all ROI contrasts and connectivity analyses.

All probe effects were transient, while all occluded period effects were sustained. Reported transient effects were based on deconvolved GLM estimates (10 time points per trial type) for each subject separately (collapsed across runs). The maximum value (the peak of the estimated hemodynamic response) for each subject for each trial type was determined, and this was subtracted by the value at the trial type's first time point. These difference values, indicating the amount of BOLD signal increase in response to the task event, were used for all transient analyses. ANOVAs including these values were non-repeated measures and included subjects as a random effect. These ANOVAs used one GLM estimate difference per region per condition per subject.

The dissociation between DLPFC and ACC/pSMA was tested using each subject's GLM estimates from each ROI in an ANOVA with subjects as a random effect. We looked for a statistically significant region by condition interaction. Conditions included the target switching occluded thirds and the non-switching occluded thirds (which were all sustained conditions). This same analysis was also run with the entire CCN (including all six rather than just two regions), with the same conditions. Different conditions (target switching foils, target switching targets, distracters, non-switching foils, and non-switching targets; i.e., all transient conditions) were used for the probe analysis looking for a region by condition interaction.

A cluster analysis was run on the target switching and non-switching occluded thirds (sustained) estimates. The clustering

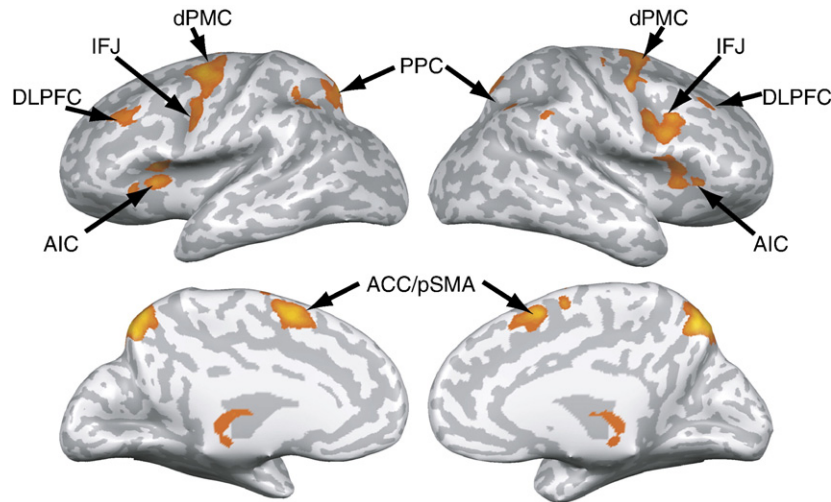


Fig. 2. The cognitive control network. Red areas on the inflated brain represent the voxels that were involved in the target switching non-occluded task relative to the non-switching non-occluded task ( $P < 0.05$ , FDR corrected). These were the regions used in the ROI analyses (see Table 1).

procedure is described in more detail below (along with the connectivity cluster analysis).

#### Functional connectivity analyses

The first functional connectivity analysis involved the following steps:

First, each CCN region (see Table 1) was selected and the preprocessed data were extracted (averaging across all voxels within a region). For comparison purposes, six additional (non-CCN) regions were also selected and their data extracted based on group functional activation during some portion of the task and evidence from previous studies suggesting domain-specific responses in these regions (see Table 2). S1 and M1 ROIs were defined by target switching (TargSw) targets vs. TargSw foils (contrasting the approximate peaks: third, fourth, and fifth time-

points). V1 and rACC were defined by TargSw targets vs. fixation (rACC showed a statistically significant negative BOLD response). Hippocampus was defined by the non-switching (NonSw) occluded period with the less frequent target ( $135^\circ$ ) vs. the NonSw occluded period with the more frequent target ( $45^\circ$ ). Broca's area was defined by TargSw occluded vs. NonSw occluded periods (overlapping with the left VLPFC region in Table 3). S1, M1, rACC, and V1 were defined by transient effects (probes), while hippocampus and Broca's area were defined by sustained effects (occluded period activation).

Second, the resting state data were selected for each region, and these time series were bandpass filtered ( $0.009 < f(\text{Hz}) < 0.08$ ) (see Cordes et al., 2001 for review of frequencies contributing to resting state correlations) after spurious variance from several sources was removed from the data using linear regression. These sources included a ventricular region (frontal horns of the lateral

Table 1  
Cognitive control network ROIs

Region	BA	T-value	P-value	Volume	Talairach
R DLPFC	9	3.059	0.004	1211	33, 33, 44
L DLPFC	9	2.990	0.004	1758	-37, 33, 37
R ACC/pSMA	6, 8	3.592	0.003	2089	4, 9, 50
L ACC/pSMA	6, 8	3.684	0.003	2903	-6, 7, 49
R dPMC	6	3.557	0.003	5274	31, -4, 58
L dPMC	6	3.502	0.003	6270	-27, -5, 55
R IFJ	6, 9	3.198	0.004	3078	42, 8, 31
L IFJ	6, 9	2.940	0.005	2354	-46, 2, 36
R AIC	13	3.137	0.004	3032	34, 18, 11
L AIC	13	3.423	0.003	3042	-33, -18, 9
R PPC	7, 40	2.846	0.006	2689	39, -53, 46
L PPC	7, 40	3.082	0.004	4193	-26, -58, 43

These regions were defined by the contrast of the target switching non-occluded period and the non-switching non-occluded period ( $P < 0.05$ , FDR corrected). The regions were combined across hemispheres for all analyses, making a total of six regions. The listed volume is in  $\text{mm}^3$ , and the  $P$ -values listed are the uncorrected  $P$ -values (though the listed voxels were restricted to those that showed  $P < 0.05$ , FDR corrected for multiple comparisons).

Table 2  
Non-CCN regions of interest

Region	BA	T-value	P-value	Volume	Talairach
L primary somatosensory (S1)	1, 2, 3	2.604	0.014	1889	-39, -30, 59
Bilateral primary visual (V1)	17	3.829	0.001	2276	-2, -89, 1
R primary motor (M1)	4	2.175	0.030	397	42, -19, 59
L Broca's Area (BA44)	44	2.465	0.018	627	-56, 11, 7
Bilateral rACC	32, 24	-6.186	0.000	3915	-4, 41, 2
L hippocampus	-	2.874	0.010	2395	-34, -17, -11

These cortical regions were used in the connectivity analyses, and were representative of the whole rest of cortex outside the CCN (see Tables 4B and C). They were defined by various contrasts. S1 and M1: target switching targets vs. target switching foils. V1 and rACC: Target switching targets vs. fixation. Broca's area: Target switching occluded vs. non-switching occluded periods. Hippocampus: The non-switching occluded period with the less practiced target ( $135^\circ$ ) vs. the non-switching occluded period with the more practiced target ( $45^\circ$ ; practiced on 25% vs. 75% of the trials, respectively).

Table 3  
Target switching occluded effects

Region	BA	T-value	P-value	Volume	Talairach
R FPC	10	2.778	0.006	320	34, 61, 6
R DLPFC	9	2.938	0.004	3199	36, 38, 34
R dPMC	6	2.973	0.004	1375	34, 2, 58
R lateral PPC	40	3.309	0.003	7044	40, -52, 41
L lateral PPC	40	2.712	0.007	605	-41, -46, 36

These are regions more active ( $P < 0.05$ , FDR corrected) for the first third of the target switching occluded period relative to the first third of the non-switching occluded period. The left DLPFC region is virtually identical to the left DLPFC ROI used in the ROI analyses and listed in Table 1, while the right DLPFC is just ventral to the right DLPFC ROI (also used in the ROI analyses) listed in Table 1. These effects could be due to working memory manipulation (switching between targets) or working memory load (two targets to maintain).

ventricles) and a region centered in the white matter (splenium of the corpus callosum), similar to the analysis performed by Fox et al. (2006). These steps are important to avoid correlations due to

cardiac (0.6 to 1.2 Hz) and respiratory signals (0.1 to 0.5 Hz), as well as various sources of magnetic resonance noise. The resting state data were used to rule out inter-regional correlations due to task performance, though the analysis was run again separately using data from target switching trials to assess if there was any difference in low frequency BOLD fluctuations during rest and task performance. An additional analysis checking for differences between rest and task performance at the higher frequencies in the data ( $0.09 < f(\text{Hz}) < 0.5$ ) involved identical steps, but with a different bandpass filter.

Third, functional connectivity was estimated using linear correlations computed for each pair of ROIs for each run separately (105 rest periods of 60 s/30 time points each). A Fisher's  $z$  transformation was then applied to the correlation parameters for each run to ensure that the correlation coefficients were normally distributed. These values were averaged, and then an inverse Fisher's  $z$  transformation was applied for reporting in Table 4.

Fourth, a non-repeated measures ANOVA with subjects as a random effect was run on the Fisher's  $z$  transformed values for

Table 4  
Innate functional connectivity within and outside the cognitive control network

	DLPFC	pSMA	dPMC	IFJ	AIC	PPC				
<b>A</b>										
<b>DLPFC</b>										
<b>pSMA</b>	<b>0.72</b>									
<b>dPMC</b>	<b>0.76</b>	<b>0.81</b>								
<b>IFJ</b>	<b>0.63</b>	<b>0.75</b>	<b>0.79</b>							
<b>AIC</b>	<b>0.69</b>	<b>0.79</b>	<b>0.71</b>	<b>0.80</b>						
<b>PPC</b>	<b>0.61</b>	<b>0.70</b>	<b>0.80</b>	<b>0.80</b>	<b>0.68</b>					
S1	0.31	0.46	0.51	0.46	0.41	0.39				
V1	0.41	0.52	0.50	0.47	0.44	0.51				
Broca's Area	0.44	0.64	0.56	0.65	0.68	0.51				
Hippocampus	0.35	0.44	0.52	0.52	0.45	0.38				
M1	0.43	0.61	0.62	0.70	0.63	0.61				
rACC	0.27	0.37	0.30	0.46	0.46	0.20				
<b>B</b>										
<i>Average connectivity to rest of CCN</i>										
DLPFC	pSMA	dPMC	IFJ	AIC	PPC	Overall				
0.68	0.75	0.78	0.76	0.73	0.72	0.74				
<i>Average connectivity to non-CCN (functionally defined) regions</i>										
DLPFC	pSMA	dPMC	IFJ	AIC	PPC	Overall				
0.37	0.51	0.50	0.54	0.51	0.43	0.48				
<b>C</b>										
	Subjects									
	1	2	3	4	5	6	7	8	9	Overall
'Within-CCN' correlations	0.66	0.61	0.90	0.59	0.74	0.65	0.82	0.55	0.64	0.71
'CCN to rest of cortex' correlations	0.37	0.44	0.70	0.48	0.55	0.39	0.61	0.39	0.33	0.49
T-values	9.1	5.5	13.5	3.4	8.1	8.7	10.8	4.7	10.4	25.3

(A) The innate functional connectivity parameters between each of the ROIs, as defined by the linear correlation during resting fixation, are listed. CCN connectivity parameters are in bold. All functional connectivity parameters were significant above zero (typically  $P < 0.00001$ ). The average connectivity across all CCN regions was  $R = 0.74$  (SD:0.06) at rest and  $R = 0.76$  (SD:0.06) during task (target switching trial) performance. (B) The average connectivity of each CCN region to the rest of the network, and the average connectivity of each non-CCN (functionally defined) region to the network. (C) Connectivity determined by the cortex-wide network delineation analysis. This analysis tested if within-CCN connectivity was higher than CCN connectivity with the *whole* rest of cortex (not just the functionally defined non-CCN regions). All subjects showed a highly significant effect (highest  $P$ -value was for subject four: 0.0007). The  $P$ -value for the group  $t$ -test was  $< 0.00001$ . Note that all averaging of correlation coefficients occurred on the  $z$ -transformed values, and an inverse  $z$  transform was then applied to that average.

each run. The  $z$  values for each run for each subject (105 per region) were sorted into either ‘within-network’ or ‘network to non-network’ categories. The ANOVA tested if within-network connectivity was statistically different than network to non-network connectivity.

Fifth, a more detailed analysis was run using a series of non-paired  $t$ -tests. Each CCN region’s average within-network connectivity was compared to that CCN region’s connectivity with each of the non-CCN regions (6 CCN regions \* 6 non-CCN regions = 36  $t$ -tests). Separate correlation coefficients for each run for each subject (105 in total) were used in these statistical tests. This analysis tested if *every* CCN region was better connected within the network than with *each* non-CCN region. Sixth, in order to assess if connectivity between CCN regions was higher than between non-CCN regions, a cluster analysis was run on the preprocessed time series used in the correlation analyses. This analysis used the default distance-based clustering in Matlab to determine if the CCN formed a cluster relative to non-CCN regions. The pairwise Euclidean distances between time series were computed first, then a hierarchy based on the proximity between each pair of time series was produced using the distance values, and finally natural groupings in the hierarchy were detected using a quantitative measure of link inconsistency (see Hogg and Ledolter, 1987). This same clustering method was used to find *DLPFC-like* and *ACC/pSMA-like* regions for the occluded thirds analysis, except that the GLM BOLD estimates (rather than the time series) were used and the analysis was limited to two clusters.

An additional convergent analysis was run in order to determine if within-network connectivity was higher than network connectivity with the rest of cortex as a whole. This approach, which we call Network Delineation Analysis, compares within-network correlations to network correlations with thousands of samples encompassing all of cortex. This analysis is important due to its inclusion of the entire cortical mantle, though its regions are not functionally defined and thus perhaps unlikely to correlate as consistently as the six non-CCN regions used in the above analysis. Thus these two analysis approaches complement each other and can together lend substantial support for the CCN’s network status.

The steps for this network delineation analysis were as follows:

First, in order to restrict the analysis to cortex, each subject’s grey-white matter boundary was determined using BrainVoyager QX’s auto-segmentation algorithm. This boundary was then expanded by 10 mm in order to encompass the subject’s grey matter, and the subcortical portions were manually removed. Each of these masks was then imported into Matlab and a linear transformation was applied to convert each mask (1 mm<sup>3</sup> per voxel) into the same coordinate space as the functional data (3 mm<sup>3</sup> per voxel). Both the mask and the functional data were already transformed into Talairach space in BrainVoyager prior to this linear transformation.

Second, each CCN region’s center point was determined and a cube of approximately the same volume as the original region (see Table 1) was selected with that point at its center. These cubes, rather than the originally defined volumes of interest, were used to ensure similarity with the non-CCN cortical samples described below. A total of 12 regions were included (one for each hemisphere for each of the six CCN regions). Voxels within each of these cubes were included if they were

within each subject’s grey matter mask. Thus, CCN regions included in this analysis tended to be smaller than those in the other analyses. White matter and ventricle voxels, used for removing spurious signals (see above), were selected in an identical manner except that all voxels within the cubes were included (no grey matter restriction).

Third, the entire brain volume was split into 3 × 3 × 3 cubic samples, each with the same volume as the median cubic CCN region volume (27.3 mm<sup>3</sup> voxels). A sample was included in the analysis if at least 50% of its voxels were within that subject’s grey matter, and if none of its voxels overlapped with voxels within the CCN cubes. Once one of these non-CCN samples was accepted, only the voxels within that subject’s grey matter were included within it. Thus, sample size varied from 14 to 27 voxels. On average, 1320 (SD: 141) non-CCN cortical samples were included per subject. Samples excluded due to overlap with CCN cubes numbered 117 per subject on average (SD: 9).

Fourth, time series were extracted from the fixation rest periods for each CCN region and non-CCN sample for each run. Each run for each subject was analyzed separately. Just as was done in the first correlation analysis, these time series were run through a regression to remove spurious signals using the ventricle and white matter samples before a bandpass filter was applied (using the same parameters as above). Pair-wise linear correlations between each CCN region and all regions (including CCN regions and non-CCN samples; excluding self-correlations) were then computed for each run. These correlation coefficients were then  $z$ -transformed. Histograms and quantile–quantile (Q-Q) plots (see Wilk and Gnanadesikan, 1968) were used to check for major deviations from the normal distribution; none was found for either the within-network or network to non-network distributions.

Fifth, a non-paired  $t$ -test was run on the set of  $z$ -transformed correlations across all subjects (see Table 4C). The correlation coefficients were separated into ‘within-network’ and ‘network to non-network’ categories for comparison. Though the means were almost identical to those in the first correlation analysis, there was considerable inter-subject variability in this analysis. This variability was likely due to differences in CCN region localization across subjects (the cubed group ROIs were probably better estimates for some subjects than others), rather than true differences in subjects’ functional connectivity. We ran a separate  $t$ -test for each subject to ensure that within-network connectivity was higher than connectivity to the rest of cortex for all subjects independently (see Table 4C).

Sixth, connectivity was assessed across all of cortex (not just with the CCN) for comparison. Cortical samples were selected as described in step three above, except that CCN regions were not excluded. All pair-wise correlations across cortex were computed separately for each run. The data were preprocessed in the same way as described above before the correlation coefficients were determined. Non-paired  $t$ -tests were computed using correlation coefficients for all runs across all subjects.

## Results

### Behavioral results

Subjects were correct 98% of the time on average (SD: 1.4%). Accuracy dropped during the occluded conditions, but remained

high at 86% (SD: 10.9%). This shows that subjects were compliant during the occluded periods, in which they had to maintain or switch the target stimulus during long blank periods with infrequent probes.

Reaction time data are only available for target trials since these were the only trials with a button response (there were not enough false alarms for inclusion in the analysis). Mean reaction time for all target trials was 552 ms. There was a significant switching effect between the switching trials and the non-switching trials. The mean RT for the non-switching trials was 533 ms, whereas the mean RT during the switching trials was 570 ms ( $F_{1,8}=12.1$ ,  $P=0.0005$ ). A non-repeated measures ANOVA with subjects as a random effect was used for this analysis.

#### Functionally identifying the CCN

The cognitive control network (CCN) was localized using voxels showing a main effect of target switching during the non-occluded periods. A contrast of the GLM fit to the non-occluded periods (target switching vs. non-switching) was used, with  $P<0.05$  (FDR corrected for multiple comparisons).

As expected, non-occluded target switching involved all of the predicted CCN areas bilaterally. This contrast provided an independent specification of the ROIs for all later analyses (see Table 1 and Fig. 2). These regions showed highly correlated activity ( $R=0.76$ ) during task performance, and were co-active during high cognitive control demands (probe processing and response set preparation; see below). This suggests that these regions form a tightly coupled network for implementing cognitive control.

#### Functional connectivity of CCN and non-CCN regions

As an independent convergent measure of CCN differentiation from the rest of cortex, we examined low frequency BOLD signal

fluctuations during resting state and task performance. Assessing correlations among these signals quantified the degree of connectivity within the CCN relative to the rest of cortex. Functional connectivity was predicted to be higher within the CCN than between CCN and non-CCN regions. Additionally, within-CCN connectivity was predicted to be higher than average connectivity between all cortical regions.

The resting state and task performance functional imaging data showed high correlations among the CCN regions. Resting state correlations were high at  $R=0.74$  on average (see Table 4). Connectivity during task performance (target switching trials;  $R=0.76$ ) was not significantly different than connectivity at rest ( $T=1.2$ ,  $P=0.22$ ) at low frequencies ( $0.009<f(\text{Hz})<0.08$ ). In contrast, at higher frequencies ( $0.09<f(\text{Hz})<0.5$ ) connectivity during task performance ( $R=0.74$ ) was greater than connectivity at rest ( $R=0.72$ ) within the CCN ( $T=6.9$ ,  $P<0.00001$ ). The lower frequencies were used for all subsequent analyses (see Materials and methods).

The resting state activity was highly correlated within the CCN compared to correlations between CCN and non-CCN active regions. The non-CCN regions were functionally defined regions outside of the CCN that showed differential activation across various task demands (see Table 2). Comparing connectivity between the CCN and non-CCN regions allowed us to assess the functional relevance of CCN connectivity relative to general connectivity across other regions involved in the visual search task. The results of a non-repeated measures ANOVA (with subjects as a random effect) revealed that the CCN regions were more connected within the network than with the non-CCN regions ( $F_{1,8}=2735$ ,  $P<0.00001$ ). A more detailed analysis found that every CCN region was individually more connected within the CCN than with each of the non-CCN regions ( $P<0.05$ , with  $P=0.0003$  on average). This detailed analysis compared each CCN region's mean connectivity within the CCN to that region's connectivity with each of the non-CCN regions using a series of  $t$ -tests (see Materials and methods).

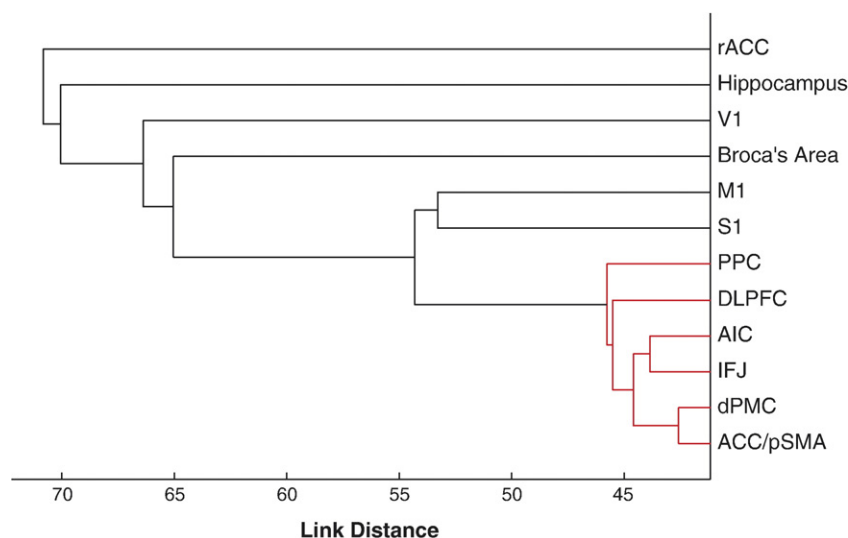


Fig. 3. Cluster plot illustrating distances between CCN and non-CCN regions. The cluster analysis was run on the preprocessed fMRI resting state data. The CCN regions form a tight cluster relative to the non-CCN regions (even relative to M1 and S1, which are known to have similar connectivity profiles). This supports the results found in the correlation analyses, and is consistent with results found for comparing CCN connectivity to the whole rest of cortex (not just these non-CCN regions; see Table 4C). The CCN links were colored red using Matlab's default criterion for cluster significance (all links in the cluster sum to less than 70% of the largest distance in the data).

In accordance with the above analyses, a distance-based cluster analysis identified the CCN as a tightly coupled network. The cluster analysis was run on the bandpass filtered CCN time courses during rest; there was much less distance between the CCN regions relative to the non-CCN regions (see Fig. 3). An example of the slow wave activity underlying the correlation and cluster analyses results is shown in Fig. 4. This example consists of the bandpass filtered time courses from all CCN and non-CCN regions for a single run (5 min) from a single subject.

An additional measure of CCN coupling was based on measuring CCN connectivity to all of cortex (rather than just the functionally defined non-CCN regions). Within-CCN correlations were compared to CCN correlations with the whole rest of cortex. The cortex was split into 27-voxel ( $\sim 1 \text{ cm}^3$ ) cubes, and those excluding all CCN voxels and including at least 50% grey matter were used as non-CCN samples (1320 used per subject on average). Mean within-CCN connectivity was  $R=0.71$ , while mean CCN to non-CCN sample connectivity was  $R=0.49$ . The similarity between CCN connectivity with the non-CCN regions ( $R=0.48$ ) and CCN connectivity with the non-CCN samples ( $R=0.49$ ) indicates that the functionally defined non-CCN regions represented the rest of cortex well.

A non-paired  $t$ -test indicated that mean within-CCN connectivity ( $R=0.71$ ) was higher than mean CCN to non-CCN sample connectivity ( $R=0.49$ ) across all of cortex ( $T=25$ ,  $P<0.00001$ ).  $T$ -tests for each subject individually indicated that every subject showed this effect ( $P<0.0001$ ; see Table 4C).

Connectivity across all of cortex (not exclusive to the CCN;  $R=0.40$ ) was below that of within-CCN connectivity ( $R=0.71$ ;  $T=32$ ,  $P<0.00001$ ) as well as that of CCN to non-CCN samples ( $R=0.49$ ;  $T=103$ ,  $P<0.00001$ ). Two of nine subjects did not show this latter effect, however, while one did not show the former (at  $P<0.05$ ). Mean cortical connectivity (pair-wise correlations across all cortical samples) was  $R=0.40$ , and a non-paired  $t$ -test indicated that the mean connectivity across cortex was greater than zero ( $T=3674$ ,  $P<0.00001$ ). All subjects showed this effect (at  $P<0.00001$ ).

This indication of significant mean connectivity across all of cortex supports the need to *compare* levels of functional connectivity within cortex, rather than simply showing connectivity greater than zero, when claiming special network status for a set of regions (the brain as a whole is a network, after all). Note that the base cortex-wide correlation of  $R=0.40$  may simply reflect signals from wide-influencing origins such as the ventral tegmental

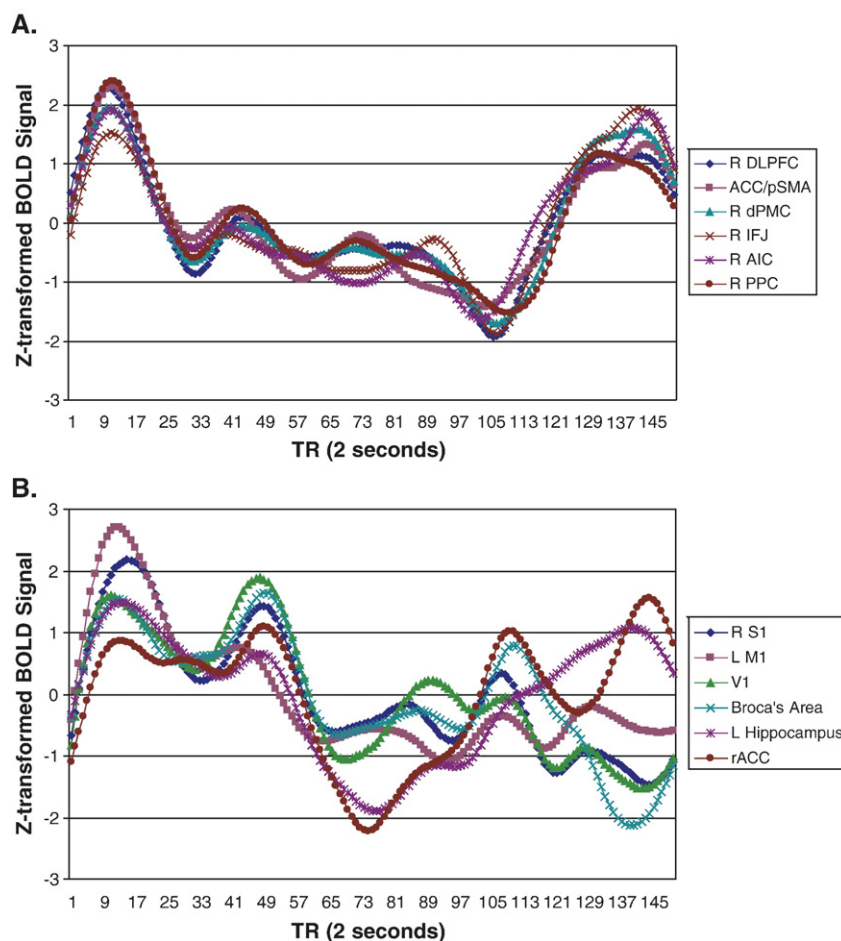


Fig. 4. Example of slow wave patterns for a single run. (A) Bandpass filtered time series for CCN regions for a single run for one subject (5 min). This covers all task conditions including non-switching, target switching, fixation rest, non-switching, and location switching, respectively. The average correlation between the CCN regions for this run was  $R=0.94$ . (B) Bandpass filtered time series for non-CCN regions for the same single run as above. The average correlation between the non-CCN regions for this run was  $R=0.58$ . The average correlation between the CCN and non-CCN regions for this run was  $R=0.29$ . This example is consistent with the differences in connectivity found between the CCN and the whole rest of cortex (see Table 4C).

area (i.e., dopamine signals) and the locus ceruleus (i.e., norepinephrine signals).

*Probe processing involves all CCN regions*

We hypothesized that all parts of the CCN would be active during demanding probe events (e.g., targets and foils). The processing of a probe requires comparing the contents of working memory with the incoming stimulus, preparing for response initiation, and performing or withholding the motor response. An ANOVA (with subjects as a random effect) including every CCN region and every transient (probe) condition did not show a significant region by condition interaction, supporting the prediction that the entire network is involved in response processing ( $F_{20,8}=0.58, P=0.92$ ). This ANOVA also showed a main effect of condition ( $F_{5,8}=15.3, P<0.0001$ ), suggesting there may be differences between probe types across the entire network (see Figs. 5 and 6).

Comparisons between target probes and distracter probes were statistically significant across the CCN, just as they were for foil probes (previous targets that had become irrelevant) relative to distracter probes (see Fig. 5A). The probe processing effects showed a similar pattern across CCN regions (i.e., TargSw

Foil>TargSw Target>Distracter). Note that distracters were combined across the target switching and non-switching conditions since they were the exact same stimuli and a direct comparison between the conditions revealed no statistically significant differences ( $F_{1,8}=2.24, P=0.14$ ). Every CCN region was significantly active for distracters relative to baseline, suggesting that the full CCN is involved in probe evaluation in general, while being additionally modulated by probe difficulty/conflict.

*Dissociation between DLPFC and ACC/pSMA*

Analysis of the occluded periods revealed the hypothesized dissociation between DLPFC and ACC/pSMA. We expected that DLPFC would show working memory effects early in the occluded periods due to active maintenance, while ACC/pSMA would not. We predicted that both regions would be involved in response set preparation late in the occluded periods, non-occluded processing, and probe processing. An ANOVA (with subjects as a random effect) including DLPFC and ACC/pSMA (bilateral) regions across each third of the target switching and non-switching occluded periods (i.e., all sustained occluded period regressors) revealed a significant region by condition interaction ( $F_{1,5,8}=2.36, P<0.05$ ). Note that this analysis removed transient probe-related

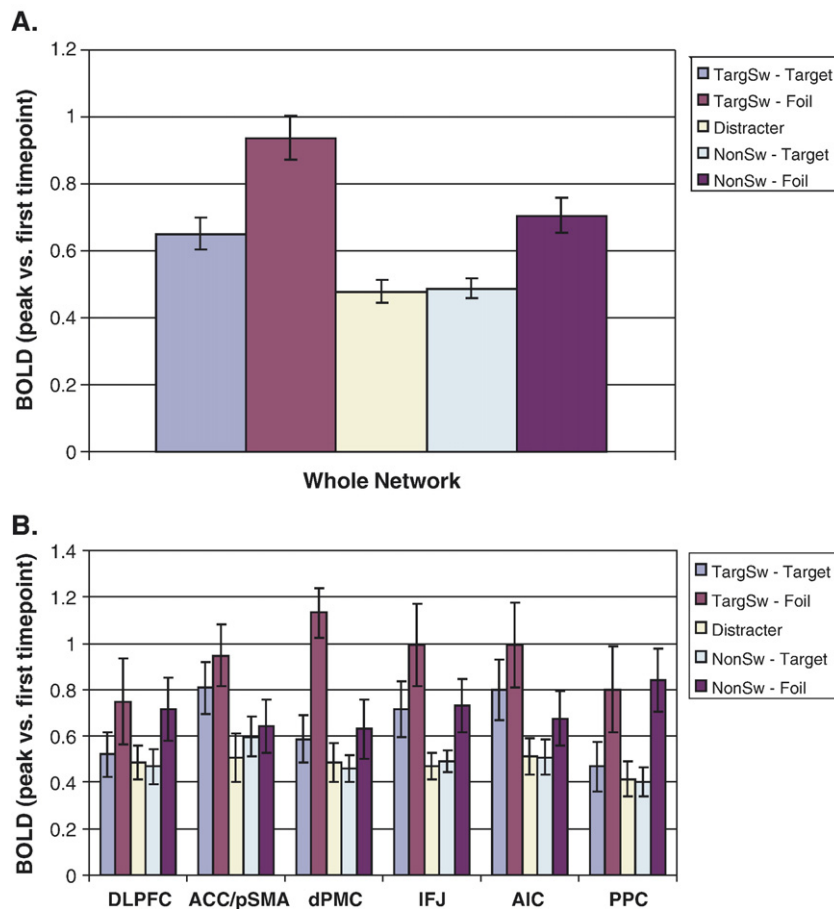


Fig. 5. Transient, probe-related activity across the cognitive control network. (A) Activity across the entire network. The regions were combined because there was no indication that the regions differed significantly across conditions (i.e., no region by condition interaction). (B) All regions showed significant increases for target switching foils relative to distracters. Note that distracters from target switching and non-switching trials were combined because there was no significant difference between them in any of the ROIs and because the same stimuli were used as distracters for both trial types.

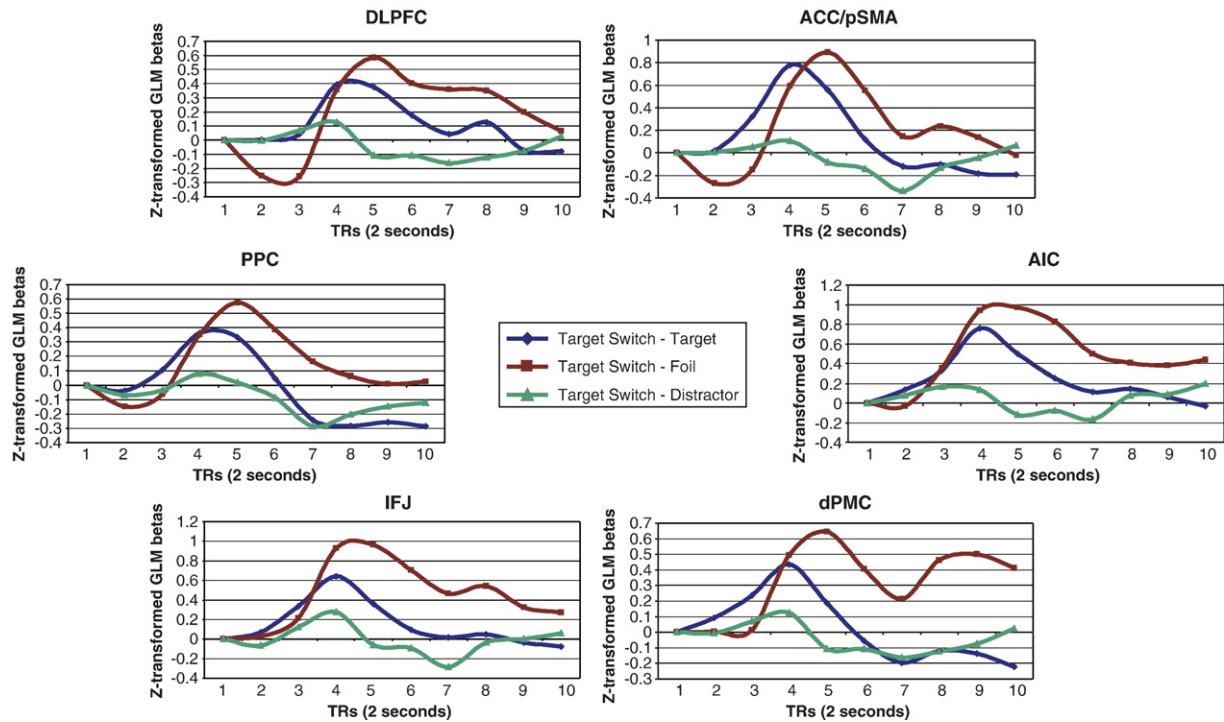


Fig. 6. Time series during target switching probes across the cognitive control network. These time series were obtained using a deconvolution GLM analysis in which each time point has a separate regressor.

activity from the sustained occluded thirds regressors (see Materials and methods).

Specific contrasts between the occluded conditions revealed several differences between the regions (see top of Fig. 7). These contrasts were run with ROI-GLMs; GLM estimates of the BOLD signal across all voxels within each ROI (as listed in Table 1). DLPFC showed a working memory effect early in the occluded periods but ACC/pSMA did not. Activity was significantly higher during the first third of the target switching occluded period relative to both fixation baseline (DLPFC:  $T=3.60$ ,  $P=0.0003$ ; ACC/pSMA:  $T=-0.10$ ,  $P=0.92$ ) and the second third of the target switching occluded period (DLPFC:  $T=2.85$ ,  $P=0.004$ ; ACC/pSMA:  $T=-1.51$ ,  $P=0.13$ ) for DLPFC only. DLPFC, not ACC/pSMA, also showed significantly higher activity for the first third of the non-switching occluded period relative to both baseline and the last third (conjunction analysis; DLPFC:  $T=2.95$ ,  $P=0.003$ ; ACC/pSMA:  $T=-0.47$ ,  $P=0.64$ ).

Both DLPFC and ACC/pSMA showed a preparatory effect late in the target switching occluded period. More precisely, both regions showed an increase in activity for the last third of the target switching occluded period relative to baseline (DLPFC:  $T=3.17$ ,  $P=0.002$ ; ACC/pSMA:  $T=4.83$ ,  $P=0.000001$ ), the second third of the target switching occluded period (DLPFC:  $T=2.93$ ,  $P=0.003$ ; ACC/pSMA:  $T=3.338$ ,  $P=0.0008$ ), and the last third of the non-switching occluded period (DLPFC:  $T=2.88$ ,  $P=0.004$ ; ACC/pSMA:  $T=3.55$ ,  $P=0.0004$ ).

Differentiation of DLPFC and ACC/pSMA functional connectivity (relative to other CCN regions) was found by clustering the resting state data (described above). As indicated in Fig. 3, the two regions have a larger distance between them than most of the CCN. This difference in connectivity patterns between the regions supports the dissociation found via the functional activations.

#### Network activity across occluded thirds

We examined specialization within the CCN during the occluded periods and identified two sets of regions within the CCN differentially related to working memory and response preparation. Expanding upon the DLPFC-ACC/pSMA dissociation, a cluster analysis was performed across all six CCN regions using the BOLD estimates from the thirds analysis GLM. With the number of clusters restricted to two, the cluster analysis revealed a cluster of regions that were *DLPFC-like* and a cluster of regions that were *ACC/pSMA-like*. DLPFC, PMC, AIC, and IFJ were in one cluster, while ACC/pSMA and PPC were in the other cluster (see Fig. 7). When lateral PPC was included, it grouped with the *DLPFC-like* regions.

These clusters were meaningful in that the *DLPFC-like* regions all showed working memory effects (activity during the first third of the occluded periods relative to baseline), while the *ACC/pSMA-like* regions did not. However, there were enough similarities between the regional activations that an analysis of cluster by condition interaction was not quite significant ( $F_{1,5,8}=1.78$ ,  $P=0.11$ ).

Splitting the working memory cluster in two, the following three categories can be used to describe the CCN regions: (1) Regions showing *working memory set up* effects, (2) Regions showing *sustained working memory* effects, and (3) Regions showing *response set preparation* effects. Category one, regions showing a significant drop from the first to second occluded target switching third, includes DLPFC ( $T=2.85$ ,  $P=0.004$ ) and lateral PPC ( $T=3.07$ ,  $P=0.002$ ). Category two, regions showing significant sustained activity across all occluded thirds relative to baseline (conjunction analysis), include dPMC (lowest:  $T=2.82$ ,  $P=0.005$ ), lateral PPC (lowest:  $T=3.40$ ,  $P=0.001$ ), and AIC (lowest:  $T=2.03$ ,  $P=0.043$ ). Category three, regions showing a

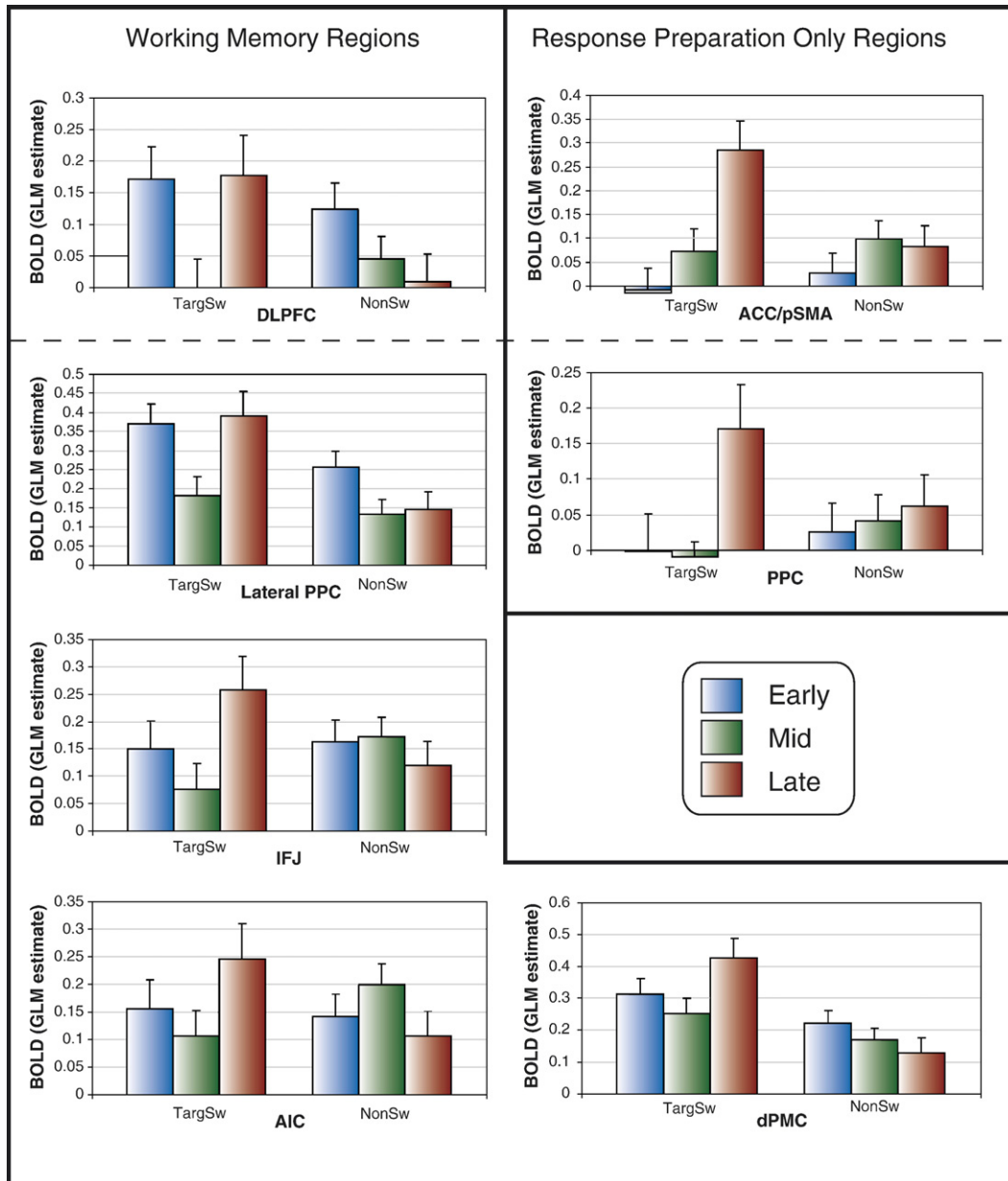


Fig. 7. Sustained occluded period effects within the cognitive control network. A cluster analysis run on the occluded thirds conditions (the occluded periods separated into thirds across time) splits the network into ‘working memory regions’ (left) and ‘response preparation only regions’ (right). All regions showed a response preparation effect, while the preparation-only cluster showed no additional working memory effect. Top portion: The dissociation between DLPFC and ACC/pSMA indicated by a significant region by condition interaction was followed up by a series of comparisons between the conditions for each region. Only DLPFC showed significant sustained activity during the first third of the occluded periods and a significant drop in that activity over the additional thirds (for both target switching and non-switching periods). Both DLPFC and ACC/pSMA showed a significant increase in activity between the second and last third of the target switching condition, and more activity in the last third of the target switching occluded period relative to the last third of the non-switching occluded period. No preparatory activity was present for non-switching trials likely because less cognitive control was necessary for non-switching probes (due to consistent S–R mapping). Bottom portion: Activity across the occluded conditions for all CCN regions, including the lateral subset of voxels within PPC (predicted to show working memory effects). Note that sustained activity shown in this figure is independent of transient, probe-related activity. TargSw=target switching trials; NonSw=non-switching trials. Each occluded third is represented by a histogram bar in its original temporal order (left to right).

significant increase for the last third of the target switching occluded period ([Last third of the target switching occluded period > Second third of target switching occluded period] and [Last third of target switching occluded period > Last third of non-switching occluded period]), include the entire CCN: ACC/pSMA ( $T=3.34$ ,  $P=0.001$ ;  $T=3.55$ ,  $P=0.000$ ), DLPFC ( $T=2.29$ ,

$P=0.003$ ;  $T=2.89$ ,  $P=0.004$ ), IFJ ( $T=2.91$ ,  $P=0.004$ ;  $T=2.23$ ,  $P=0.026$ ), dPMC ( $T=2.23$ ,  $P=0.026$ ;  $T=4.02$ ,  $P=0.000$ ), AIC ( $T=2.49$ ,  $P=0.01$ ;  $T=2.53$ ,  $P=0.012$ ), PPC ( $T=3.11$ ,  $P=0.001$ ;  $T=2.07$ ,  $P=0.038$ ), and lateral PPC ( $T=3.24$ ,  $P=0.001$ ;  $T=3.48$ ,  $P=0.001$ ). There was a main effect of condition (occluded thirds) across the entire network ( $F_{5,8}=8.84$ ,  $P<0.00001$ ), supporting the

conclusion that all of the CCN regions were involved in preparatory activity in the last third of the target switching occluded period. All of these statistical tests used ROI-GLM estimates of BOLD signals (see Table 1 for ROI locations). See Materials and methods for details on how conjunction analyses were conducted.

#### *Voxel-wise analyses across working memory conditions*

Voxel-wise contrasts across the entire brain were performed in order to discover effects in regions not included in our ROI analyses. The first third of the target switching occluded period was contrasted with the first third of the non-switching occluded period, revealing a series of regions overlapping with several CCN regions, including DLPFC (see Table 3). The left DLPFC region showing this occluded target switching effect was identical to the left DLPFC ROI chosen for the main ROI analysis, while the right DLPFC region was several millimeters ventral to the right DLPFC ROI chosen for the ROI analysis.

The significant decrease seen in DLPFC during target maintenance and switching was explored using the voxel-wise conjunction of two contrasts: first vs. second third of the target switching occluded period, and the first vs. second third of the non-switching occluded period. This contrast revealed right DLPFC, anterior dPMC, and lateral PPC activation (see Table 5). The lateral PPC activation was of particular interest because this region was in a similar location to PPC regions showing working memory effects in previous studies (e.g., Barch et al., 1997; Braver et al., 1997; D'Esposito et al., 1999), and also because it showed such a different set of effects relative to the entire PPC region (which included precuneus) used in the main ROI analysis. As described above, the lateral portion of the PPC ROI (separated from precuneus) showed a pattern of activity very similar to DLPFC.

The preparatory effect during the last third of the target switching occluded period was present for all of the CCN regions (see Fig. 7). A voxel-wise analysis using the conjunction of two contrasts (last third of the target switching occluded period vs. the second third of the target switching occluded period, and last third of the target switching occluded period vs. the last third of the non-switching occluded period) revealed voxels within each CCN region, in addition to several regions outside the CCN (see Table 6). These

Table 5  
Working memory drop-out effects

Region	BA	T-value	P-value	Volume	Talairach
L FPC	10	2.426	0.016	594	-41, 49, 3
R DLPFC	9	2.434	0.016	645	38, 41, 32
L DLPFC	9	2.431	0.016	239	-41, 32, 35
L VLPFC	44	2.605	0.012	577	-56, 14, 8
R dPMC	6	2.687	0.011	1026	34, 0, 60
L dPMC	6	2.669	0.010	1619	-28, -8, 57
L AIC	13	2.328	0.020	87	-34, 17, 11
L PPC	7	2.613	0.011	1455	-25, -63, 53
R lateral PPC	40, 7	2.617	0.011	1677	48, -42, 45
L lateral PPC	40, 7	2.965	0.008	5315	-44, -45, 47

These are regions more active ( $P < 0.05$ , FDR corrected) for the first third relative the second third for both target switching and non-switching occluded periods. FPC=fronto-polar cortex.

Table 6  
Voxel-wise preparatory effects

Region	BA	T-value	P-value	Volume	Talairach
ACC/pSMA	8, 6	3.727	0.0002	629	4, 8, 54
R DLPFC	9, 10	3.775	0.0002	1133	37, 39, 36
<i>L DLPFC</i>	<i>9, 10</i>	<i>2.550</i>	<i>0.0120</i>	<i>1570</i>	<i>-38, 44, 21</i>
R inferior DLPFC	46	3.721	0.0002	121	48, 49, 15
R VLPFC	47	3.559	0.0004	83	50, 16, 0
<i>R IFJ</i>	<i>9</i>	<i>2.787</i>	<i>0.0075</i>	<i>1982</i>	<i>40, 9, 23</i>
R PMC	6	3.700	0.0002	1047	43, 4, 52
R AIC	13	3.553	0.0004	33	35, 13, 19
R PPC	40, 7	4.013	0.0001	1092	44, -56, 52
<i>L PPC</i>	<i>40, 7</i>	<i>2.574</i>	<i>0.0116</i>	<i>1210</i>	<i>-35, -49, 37</i>

Only voxels which increased during the last third of the occluded target switching period relative to both the previous third and the last third of the occluded non-switching period are reported. Contrast: The conjunction of the last third of the target switching occluded period vs. the last third of the non-switching occluded period, and the last third of the target switching occluded period vs. the preceding (second) third of that same period. Threshold:  $P < 0.05$ , FDR corrected for the conjunction map. The italicized regions were significant at a lower threshold of  $P < 0.05$ , with a 50 voxel cluster threshold.

additional regions included right ventrolateral prefrontal cortex and right inferior DLPFC (BA 46).

## Discussion

In the present study, we hypothesized that a set of cortical regions consistently co-active during cognitive control tasks forms a network (the CCN). We used resting state correlations to characterize and compare functional connectivity within this proposed network. Results showed that the CCN regions were better correlated within the network than to regions outside the network, indicating that calling this set of regions a 'network' is meaningful in the context of the network that constitutes the brain.

We also hypothesized that two components of this network, DLPFC and ACC/pSMA, would be dissociated between working memory and preparatory demands. Results showed that DLPFC was involved in working memory maintenance early on during the occluded delay periods, while ACC/pSMA was only involved in preparation for probe onset late in the target switching occluded periods (the point at which the anticipated need for cognitive control was highest). We also found that clustering resting state data showed differentiation of DLPFC and ACC/pSMA relative to other CCN regions (see Fig. 3).

Probe events, which involved a number of tightly coordinated cognitive processes, were predicted to involve the entire CCN. Results showed that all probes, even distracters (which were consistently irrelevant to task performance), caused activity within the entire network. Target switching foils (previous targets) and targets (previous foils) showed increased activity across the CCN, supporting our hypothesis that these probe types would be especially demanding for cognitive control processes due to negative priming.

#### *High functional connectivity between cognitive control regions*

A consensus has emerged from across many studies indicating that a common set of regions is involved in many cognitive control demands (see Wager et al., 2004; Brass et al., 2005 for review).

These regions include DLPFC, ACC/pSMA, dPMC, IFJ, AIC, and PPC. The specific location of this set of cognitive control regions was defined here by target switching demands during a visual line search task (see Figs. 1B and 2).

The co-activation of this set of regions across a large number of studies is suggestive, but not conclusive, of network status. Stephan (2004) illustrated that mutual correlation with a task regressor does not imply direct correlation between the regions, meaning that co-activation does not imply interaction. We utilized direct correlations between the cognitive control regions to determine if the regions truly interacted. Correlations were computed on resting state data in order to rule out any task-specific effects on regional correlations. The within-CCN correlations did not differ between task performance and rest, however.

The brain is a highly integrated network (especially the cortical system), such that looking for all statistically significant correlations greater than zero will often reveal connections no more functionally relevant than the basic connectivity found across the entire brain. The present study uses connectivity with regions outside the network, rather than zero, to define a null correlation distribution. This approach acknowledges that the cortical system is highly integrated to begin with ( $R=0.40$ , according to our calculations), and therefore the term ‘cortical network’ should refer to connectivity that is higher than connectivity across the cortical system as a whole.

Correlations were high between the cognitive control regions during rest ( $R=0.74$  on average), and were also high during task performance ( $R=0.76$ , SD: 0.06). We found that these correlations were meaningful in the context of the brain as a whole by comparing connectivity with six regions hypothesized to be outside the network with connectivity within the network (see Table 4). Not only was overall connectivity higher within the network than between the non-CCN regions and the CCN regions ( $P<0.00001$ ), but each CCN region was better connected on average to other CCN regions than to each non-CCN region individually ( $P<0.05$ ).

Further, within-CCN connectivity was compared to the whole rest of cortex and this also revealed that within-CCN connectivity was higher than CCN to non-CCN connectivity ( $P<0.00001$ ; see Table 4C). Pair-wise connectivity across all of cortex (including both CCN and non-CCN regions) was also lower on average than within-CCN connectivity ( $P<0.00001$ ), though this cortex-wide connectivity was also lower than CCN to non-CCN connectivity ( $P<0.00001$ ). This indicates that, on average, the CCN is better connected to the rest of cortex than other cortical regions, which is in accordance with its role in cognitive control and the resulting need to monitor and control a wide variety of cognitive processes across cortex.

We propose a novel set of converging criteria for using the term ‘network’ for brain regions. First, the regions should tend to be active together in a consistent set of task contexts. Second, the regions should be significantly correlated during both rest and task performance (indicating functional connectivity). Third, within-network connectivity should be significantly higher than the network’s connectivity with either functionally defined regions outside the network or with a large sample of randomly selected areas across cortex (ideally encompassing all of cortex). In the present study both approaches were used, indicating very similar results (functionally defined  $R=0.48$ ; randomly sampled  $R=0.49$ ; all subjects showed greater within-network connectivity with both approaches).

In trying to understand function in a tightly coupled network, the present results demonstrate the value of focusing on both similarities (e.g., during S–R processing) and differences (e.g., during working memory processing) among the regions such that more constraints are brought to bear on theoretical interpretations of the data. The present results can support a model where working memory and decision making processes are located in disparate anatomical structures that are tightly coupled to enable S–R processing. Decision difficulty may directly impact decision processes in ACC/pSMA, but the decision may require working memory traces in other areas (e.g., DLPFC, lateral PPC) resulting in multiple CCN areas showing difficulty effects, just as we observed for targets and foils relative to distracters. Most publications stress differential results, but to characterize the operations of the CCN accounting for both commonality and differential effects among its components provides an important perspective on the specialization and synergy of the interacting components of the CCN.

#### *DLPFC, ACC/pSMA dissociation*

A region by condition (occluded thirds) interaction was statistically significant for DLPFC and ACC/pSMA ( $P<0.05$ ), demonstrating a dissociation between the regions. DLPFC was active during the first third of the occluded delay period, while ACC/pSMA was not. Both regions were active during the last third of the target switching occluded period. These results suggest that DLPFC is involved in active maintenance of information, while both DLPFC and ACC/pSMA are involved in preparatory processes prior to expected probe onset (at the end of each target switching occluded period).

Rather than a general preparatory process prior to any probe, the regions were active only prior to target switching probe onset. The regions were not active prior to non-switching probe onset likely because less cognitive control was necessary for non-switching probes. It is well established that varied mapping of S–R associations forces controlled cognitive processing, while consistent mapping of S–R associations allows for automatic cognitive processing (Schneider and Shiffrin, 1977; Shiffrin and Schneider, 1977; see Chein and Schneider, 2005). Since the S–R associations did not change over the many probes presented in each non-switching trial, non-switching probes were processed in a largely automatic manner. However, controlled processing was necessary for target switching probes since the S–R associations were repeatedly varied. This in turn drove the preparatory activity in anticipation of using that controlled processing to respond appropriately to the upcoming target switching probe. Supporting this controlled vs. automatic distinction, non-switching probe reaction times (mean: 533 ms) were significantly faster than target switching probe reaction times (mean: 570 ms;  $P=0.0005$ ).

The most cited case of a DLPFC, ACC/pSMA dissociation to date is MacDonald et al. (2000). The present study’s results are largely inconsistent with that study’s conclusions. MacDonald et al. found that only DLPFC responded differentially to a high control preparatory cue, while both DLPFC and ACC/pSMA were involved in high control preparation in the present study. Note that their data showed similar increases relative to baseline during preparation and S–R processing in both regions (see Fig. 1 of MacDonald et al., 2000), supporting a conclusion that both regions were involved during both conditions. The present study’s results agree with a recent study by Brown and Braver (2005), which found that high control preparation for a response mapping task involved both

DLPFC and ACC/pSMA. Results were more similar between MacDonald et al. and the present study for the probe events, in that ACC/pSMA (not DLPFC) was more active for target switching (high control) relative to non-switching (low control) targets. It is not clear that there is a dissociation here, however, since there was no significant region by condition interaction. MacDonald et al. did not perform this statistical test, so it is unclear how statistically significant their dissociation was. Also, the foil probes in the present study show that there is a conflict effect in DLPFC (and all six CCN regions), and not just in ACC/pSMA as reported by MacDonald et al.

#### *Network integration during probe evaluation*

There were no differences between the cognitive control regions across the probe conditions. This was verified with an ANOVA showing no statistically significant region by condition interaction. There was a main effect of condition across all regions, however. All regions were more active during target switching foils relative to distracters (see Fig. 5A). The unity of the network across probe events supports our conclusion from the connectivity analysis that the cognitive control regions form a functionally integrated network.

We expected to find the entire network active in response to target switching foils and targets because the network, which has been characterized as a network specialized for cognitive control processing (Schneider and Chein, 2003), would be most tasked by cognitive control demands during these events. The entire network also responded to distracters, however. This result is consistent with a recent study by Hon et al. (2006), which showed that much of the CCN (excluding AIC and DLPFC) responded to attended changes in stimulus properties independent of task relevance.

Network activation during stimuli irrelevant to the task (i.e., distracters) suggests that the network is involved in the strategic evaluation of all probe stimuli. As this evaluation process was prolonged due to response selection difficulty (i.e., target switching foils and targets), so too did network activity increase. Both target switching foils and targets involved response conflict due to negative priming (the previous target became a foil, and vice versa), driving the need for cognitive control (Botvinick et al., 2001; Schneider and Chein, 2003) and the duration/intensity of the evaluative process.

Network activation was strongest for foils, likely because there was no discrete end to the evaluative process (e.g., a button press, as was present for targets) such that evaluation could potentially be prolonged until the next probe. In other words, the lack of a motor response during foils allowed the response selection process to continue in an undecided/evaluative state for some time without decreasing task accuracy. Konishi et al. (1998, 1999) showed a similar effect in which ACC/pSMA, DLPFC, and PPC responded to no-go trials more than go trials. Similarly, Braver et al. (2001) demonstrated an effect in these same regions in which there were significantly larger activations for response inhibition than stimulus detection or response selection. Unlike Braver et al., however, these regions were active here even during the more frequent (75% of probes) responses (i.e., no button press). This supports the interpretation that the CCN activity during foils was due to extended evaluative processes in the face of stimulus–response conflict, rather than the need to inhibit response prepotency per se.

Probe evaluation likely consists of a number of highly integrated cognitive processes. These include stimulus perception, working

memory retrieval, probe-target comparison, response preparation, and response initiation. These processes, which occur in nearly every study of cognition, are likely distributed across the components of the CCN, but are very rarely dissociated since they are so tightly coupled in time. There is perhaps little hope for dissociating these neural processes using standard methods with low temporal resolution techniques such as fMRI, though faster techniques such as magnetoencephalography may have a better chance.

#### *Characterizing the network across working memory conditions*

A number of studies have shown sustained working memory effects within DLPFC (e.g., Barch et al., 1997; D'Esposito et al., 1999; Ranganath and D'Esposito, 2001). Most of these studies used very short (~7 s) delay periods, however, leaving open the possibility that DLPFC activity may drop out over time. The present study, which had delays lasting 32 s, found that DLPFC was not active during the entire delay periods. Early and late DLPFC occluded period activity suggests that delay period processing in DLPFC is due to two processes: working memory set up and response set preparation.

The dropout of DLPFC during occluded processing between the early and middle third (see Fig. 7) suggests that DLPFC is not necessarily specialized for active maintenance, but rather for converting stimuli into sustainable memory traces according to task goals, and also for converting memory traces into actionable representations for task performance. Supporting these two roles for DLPFC, Quintana and Fuster (1999) found using single-unit recording in non-human primates that DLPFC activity dropped down over time during spatial working memory delays, while activity within a separate (but overlapping in cortical space) set of neurons within DLPFC began increasing if the need to respond was predictable. Also similar to the present study, Quintana and Fuster found that, unlike in DLPFC, activity was constant within lateral PPC during the delay period.

Similar to DLPFC and PPC, sustained working memory effects have been found within ACC/pSMA as well (e.g., Petit et al., 1998; Haxby et al., 2000). Results from the present study suggest that these working memory effects are due solely to preparation for the upcoming probe event (present just after the delay for every working memory study). The preparatory effect was only present for the target switching condition, suggesting that the additional switching or probe difficulty increased the need for preparatory processes. These processes are likely present in most working memory studies, however, since the S–R mappings shift on nearly every trial. For instance, a delayed match to sample task will typically show a stimulus that maps to button one (a match), before mapping to button two (a non-match) on the next presentation of that stimulus. Such S–R mapping inconsistency is the hallmark of cognitive control tasks (Shiffrin and Schneider, 1977), making the typical working memory task likely to involve preparatory processes to utilize controlled processing after each delay period. Working memory effects within ACC/pSMA are therefore likely to be related to preparatory activity, though such activity is likely absent when probe-related processes require relatively little cognitive control. This is consistent with the lack of activity for non-switching preparation in the present study and the drop out of activity in other studies as consistent S–R mapping tasks become automatic due to extensive practice (Chein and Schneider, 2005).

Several regions, including dPMC, lateral PPC, and AIC, showed activity sustained over all occluded thirds relative to

baseline. This activity may be due to active maintenance of task-relevant information, as such activity is typically interpreted, or this activity could be due to sustained arousal during the occluded period. This latter possibility is enhanced for the occluded line search task since there was always a possibility of probe onset throughout the entire occluded period. There seems to be little evidence in the literature for AIC activity during working memory delays, suggesting that this region may be related to sustained arousal during this period. Several studies have found that AIC responds to emotionally arousing stimuli, supporting this hypothesis (Bornhove et al., 2002; Schienle et al., 2002; see Wager and Barrett, 2004 for review). Lateral PPC and dPMC, however, are often reported as active during working memory delays (e.g., Constantinidis and Steinmetz, 1996; D'Esposito et al., 1998; Todd and Marois, 2004). This suggests that the memory trace was actively maintained within these regions across the occluded period, perhaps as 'slave' systems after being set up by a controller (DLPFC) early in the delay period.

#### *A network for cognitive control*

As mentioned above, many studies have reported activity in all or most of the cognitive control regions reported in the present study. Though the co-active regions during cognitive control tasks are quite consistent, all of the regions considered part of the CCN here are not always present across studies. Wager et al. (2004) found, using a meta-analytic statistical analysis, activation within the entire CCN (with IFJ and dPMC combined as 'PMC') across a large number of studies. However, Wager et al. did not find all CCN regions active in all studies. This may be due to a number of reasons, such as different effect sizes for different regions (e.g., IFJ and AIC tended to have relatively small effect sizes in the present study), or variation of region location across subjects. In other contexts, this may be due to different statistical thresholds used in different studies, or reporting limited to a priori regions of interest not including the entire CCN. Another compelling possibility is that differences in CCN activation between studies represent dissociations within the network (much like the dissociation found in the present study between DLPFC and ACC/pSMA), though such dissociations must be clearly demonstrated within a single group of subjects to be verified.

Note that the present study used an especially sensitive method (block design with fixed effects on group data) to localize the CCN voxels, and another sensitive method to test hypotheses regarding these regions (ROI analysis with subjects as a random effect). Thus, studies failing to show the entire CCN with voxel-wise analyses may reflect false negatives due to lack of sensitivity inherent in the method. See Table 6 for an example of how a subtle difference in statistical threshold for a voxel-wise analysis can alter reporting of activity within the CCN (an ROI analysis confirmed that the entire CCN was active for this contrast).

Dosenbach et al. (2006) found that the majority of the CCN (excluding dPMC) responded to various cognitive control demands. They emphasized ACC/pSMA and AIC as "core" cognitive control regions as these were the only two regions to respond to all of their cognitive control demands. We also found that these regions were involved in most cognitive control demands, though all of the other regions were involved as well (excluding the ACC/pSMA and DLPFC dissociation).

Of particular interest was the finding by Dosenbach et al. that activity in ACC/pSMA, not DLPFC, was sustained during task

performance. This result is seemingly inconsistent with a large body of evidence for DLPFC in working memory maintenance (e.g., Barch et al., 1997; D'Esposito et al., 1999; Ranganath and D'Esposito, 2001). Results from the present study suggest that working memory processes in DLPFC may have been present early in task performance but dropped out (see Fig. 7). The sustained regressors used by Dosenbach et al. may have failed to reach significance not because of a lack of DLPFC activity related to task maintenance, but because such activity was not sustained throughout the task blocks. In other words, DLPFC may be necessary for task maintenance early on before this information is 'downloaded' into other regions for sustained task performance.

The sustained ACC/pSMA activity found by Dosenbach et al. was likely due to preparatory processes which 'filled the gap' between probe events. Unlike the present study, the tasks used by Dosenbach et al. all had rapid probe presentation throughout the block period. The present study showed that sustained ACC/pSMA activity was present in preparation for probes (see Fig. 7), a process which could occur between rapidly presented probe events creating an illusion of a sustained process when in fact several discrete processes are involved.

Chein and Schneider (2005) found that the CCN (excluding IFJ) was involved early in practice across a large variety of tasks, but dropped out with further practice. This is consistent both with the role of the CCN in cognitive control (as automaticity builds with practice, so should the need for cognitive control decrease), and also with the drop-out effects observed in the present study. Chein et al. showed these effects over minutes and hours, though the present study found them within DLPFC and lateral PPC over seconds. The present study found significant decreases across the network over minutes for target switching foils and non-switching foils (see Fig. 5A); the same stimuli were presented in these two different contexts, yielding different responses within the network due to a learned decrease in response conflict. The present study extends the results of Chein et al., illustrating that learning can decrease CCN activity over much shorter time scales than was found in that study.

Co-activation of the CCN in response to probes (see Fig. 5) suggests that CCN regions interact during S–R processing, but it is unclear what role of each region has. It is likely that DLPFC, which we have suggested is a task/working memory controller (Schneider and Chein, 2003), is involved in converting task-relevant working memory traces into representations useful for probe evaluation, possibly via other regions (e.g., lateral PPC) which project to ACC/pSMA. ACC/pSMA, in turn, monitors target–stimulus comparison conflict as probes are evaluated and signals DLPFC to boost CCN activity as necessary. This system forms a feedback loop such that attending to the target–stimulus comparison longer (e.g., foils vs. targets) will increase activity in all components of the system.

The present results show tightly coupled processing in six regions making up the proposed cognitive control network, as well as specialization between components of that network. Cortical regions specialized for working memory and decision/response preparation support the upcoming S–R processes, which require all components of the network for successful task performance. Given the ubiquity of CCN activation across many cognitive control tasks, understanding the coordinated operation and specialization of the CCN's components is a key issue in understanding brain processing in a variety of situations.

## Acknowledgments

This work was funded by a grant from the Office of Naval Research (N00014-01-10677). The authors wish to thank Eliezer Kanak, Scott Kurdilla, and Becca Smith for technical support.

## References

- Barch, D.M., Braver, T.S., Nystrom, L.E., Forman, S.D., Noll, D.C., Cohen, J.D., 1997. Dissociating working memory from task difficulty in human prefrontal cortex. *Neuropsychologia* 35 (10), 1373–1380.
- Bornhovd, K., Quante, M., Glauche, V., Bromm, B., Weiller, C., Buchel, C., 2002. Painful stimuli evoke different stimulus-response functions in the amygdala, prefrontal, insula and somatosensory cortex: a single-trial fMRI study. *Brain* 125 (Pt. 6), 1326–1336.
- Botvinick, M.M., Braver, T.S., Barch, D.M., Carter, C.S., Cohen, J.D., 2001. Conflict monitoring and cognitive control. *Psychol. Rev.* 108 (3), 624–652.
- Brass, M., Derrfuss, J., Forstmann, B., von Cramon, D.Y., 2005. The role of the inferior frontal junction area in cognitive control. *Trends Cogn. Sci.* 9 (7), 314–316.
- Braver, T.S., Cohen, J.D., Nystrom, L.E., Jonides, J., Smith, E.E., Noll, D.C., 1997. A parametric study of prefrontal cortex involvement in human working memory. *NeuroImage* 5 (1), 49–62.
- Braver, T.S., Barch, D.M., Gray, J.R., Molfese, D.L., Snyder, A., 2001. Anterior cingulate cortex and response conflict: effects of frequency, inhibition and errors. *Cereb. Cortex* 11 (9), 825–836.
- Brown, J.W., Braver, T.S., 2005. Learned predictions of error likelihood in the anterior cingulate cortex. *Science* 307 (5712), 1118–1121.
- Cabeza, R., Nyberg, L., 2000. Imaging cognition II: an empirical review of 275 PET and fMRI studies. *J. Cogn. Neurosci.* 12 (1), 1–47.
- Chein, J.M., Schneider, W., 2005. Neuroimaging studies of practice-related change: fMRI and meta-analytic evidence of a domain-general control network for learning. *Brain Res. Cogn. Brain Res.* 25 (3), 607–623.
- Constantinidis, C., Steinmetz, M.A., 1996. Neuronal activity in posterior parietal area 7a during the delay periods of a spatial memory task. *J. Neurophysiol.* 76 (2), 1352–1355.
- Cordes, D., Haughton, V.M., Arfanakis, K., Wendt, G.J., Turski, P.A., Moritz, C.H., Quigley, M.A., Meyerand, M.E., 2000. Mapping functionally related regions of brain with functional connectivity MR imaging. *AJNR Am. J. Neuroradiol.* 21 (9), 1636–1644.
- Cordes, D., Haughton, V.M., Arfanakis, K., Carew, J.D., Turski, P.A., Moritz, C.H., Quigley, M.A., Meyerand, M.E., 2001. Frequencies contributing to functional connectivity in the cerebral cortex in resting-state data. *AJNR Am. J. Neuroradiol.* 22 (7), 1326–1333.
- D’Esposito, M., Aguirre, G.K., Zarahn, E., Ballard, D., Shin, R.K., Lease, J., 1998. Functional MRI studies of spatial and nonspatial working memory. *Brain Res. Cogn. Brain Res.* 7 (1), 1–13.
- D’Esposito, M., Postle, B.R., Ballard, D., Lease, J., 1999. Maintenance versus manipulation of information held in working memory: an event-related fMRI study. *Brain Cogn.* 41 (1), 66–86.
- Dosenbach, N.U., Visscher, K.M., Palmer, E.D., Miezin, F.M., Wenger, K.K., Kang, H.C., Burgund, E.D., Grimes, A.L., Schlaggar, B.L., Petersen, S.E., 2006. A core system for the implementation of task sets. *Neuron* 50 (5), 799–812.
- Duncan, J., Owen, A.M., 2000. Common regions of the human frontal lobe recruited by diverse cognitive demands. *Trends Neurosci.* 23 (10), 475–483.
- Fox, M.D., Corbetta, M., Snyder, A.Z., Vincent, J.L., Raichle, M.E., 2006. Spontaneous neuronal activity distinguishes human dorsal and ventral attention systems. *Proc. Natl. Acad. Sci. U. S. A.* 103 (26), 10046–10051.
- Genovese, C.R., Lazar, N.A., Nichols, T., 2002. Thresholding of statistical maps in functional neuroimaging using the false discovery rate. *NeuroImage* 15 (4), 870–878.
- Golanov, E.V., Yamamoto, S., Reis, D.J., 1994. Spontaneous waves of cerebral blood flow associated with a pattern of electrocortical activity. *Am. J. Physiol.* 266 (1 Pt. 2), R204–R214.
- Haxby, J.V., Petit, L., Ungerleider, L.G., Courtney, S.M., 2000. Distinguishing the functional roles of multiple regions in distributed neural systems for visual working memory. *NeuroImage* 11 (5 Pt. 1), 380–391.
- Hogg, R.V., Ledolter, J., 1987. *Engineering Statistics*. MacMillan.
- Hon, N., Epstein, R.A., Owen, A.M., Duncan, J., 2006. Frontoparietal activity with minimal decision and control. *J. Neurosci.* 26 (38), 9805–9809.
- Konishi, S., Nakajima, K., Uchida, I., Sekihara, K., Miyashita, Y., 1998. No-go dominant brain activity in human inferior prefrontal cortex revealed by functional magnetic resonance imaging. *Eur. J. Neurosci.* 10 (3), 1209–1213.
- Konishi, S., Nakajima, K., Uchida, I., Kikyo, H., Kameyama, M., Miyashita, Y., 1999. Common inhibitory mechanism in human inferior prefrontal cortex revealed by event-related functional MRI. *Brain* 122 (Pt. 5), 981–991.
- Lancaster, J.L., Woldorff, M.G., Parsons, L.M., Liotti, M., Freitas, C.S., Rainey, L., Kochunov, P.V., Nickerson, D., Mikiten, S.A., Fox, P.T., 2000. Automated Talairach atlas labels for functional brain mapping. *Hum. Brain Mapp.* 10 (3), 120–131.
- Luks, T.L., Simpson, G.V., Feiwell, R.J., Miller, W.L., 2002. Evidence for anterior cingulate cortex involvement in monitoring preparatory attentional set. *NeuroImage* 17 (2), 792–802.
- Luks, T.L., Simpson, G.V., Dale, C.L., Hough, M.G., 2007. Preparatory allocation of attention and adjustments in conflict processing. *NeuroImage* 35 (2), 949–958.
- MacDonald, A.W., Cohen, J.D., Stenger, V.A., Carter, C.S., 2000. Dissociating the role of the dorsolateral prefrontal and anterior cingulate cortex in cognitive control. *Science* 288 (5472), 1835–1838.
- Malley, G.B., Strayer, D.L., 1995. Effect of stimulus repetition on positive and negative identity priming. *Percept. Psychophys.* 57 (5), 657–667.
- Manoach, D.S., Schlag, G., Siewert, B., Darby, D.G., Bly, B.M., Benfield, A., Edelman, R.R., Warach, S., 1997. Prefrontal cortex fMRI signal changes are correlated with working memory load. *NeuroReport* 8 (2), 545–549.
- Nichols, T., Brett, M., Andersson, J., Wager, T., Poline, J.B., 2005. Valid conjunction inference with the minimum statistic. *NeuroImage* 25 (3), 653–660.
- Ogawa, S., Tank, D.W., Menon, R., Ellermann, J.M., Kim, S.G., Merkle, H., Ugurbil, K., 1992. Intrinsic signal changes accompanying sensory stimulation: functional brain mapping with magnetic resonance imaging. *Proc. Natl. Acad. Sci. U. S. A.* 89 (13), 5951–5955.
- Petit, L., Courtney, S.M., Ungerleider, L.G., Haxby, J.V., 1998. Sustained activity in the medial wall during working memory delays. *J. Neurosci.* 18 (22), 9429–9437.
- Quintana, J., Fuster, J.M., 1999. From perception to action: temporal integrative functions of prefrontal and parietal neurons. *Cereb. Cortex* 9 (3), 213–221.
- Ranganath, C., D’Esposito, M., 2001. Medial temporal lobe activity associated with active maintenance of novel information. *Neuron* 31 (5), 865–873.
- Schienze, A., Stark, R., Walter, B., Blecker, C., Ott, U., Kirsch, P., Sammer, G., Vaitl, D., 2002. The insula is not specifically involved in disgust processing: an fMRI study. *NeuroReport* 13 (16), 2023–2026.
- Schneider, W., Chein, J.M., 2003. Controlled and automatic processing: behavior, theory, and biological mechanisms. *Cogn. Sci.* 27 (3), 525–559.
- Schneider, W., Shiffrin, R., 1977. Controlled and automatic human information processing: I. Detection search, and attention. *Psychol. Rev.* (84), 1–66.
- Schneider, W., Eshman, A., Zuccolotto, A., 2002. *E-Prime: A User’s Guide*. Psychology Software Tools, Pittsburgh, PA.
- Schumacher, E.H., Cole, M.W., D’Esposito, M., 2007. Selection and maintenance of stimulus-response rules during preparation and performance of a spatial choice-reaction task. *Brain Res.* 1136 (1), 77–87.

- Shiffrin, R., Schneider, W., 1977. Controlled and automatic human information processing: II. Perceptual learning, automatic attending and a general theory. *Psychol. Rev.* 84 (2), 127–190.
- Smith, E.E., Jonides, J., Marshuetz, C., Koeppel, R.A., 1998. Components of verbal working memory: evidence from neuroimaging. *Proc. Natl. Acad. Sci. U. S. A.* 95 (3), 876–882.
- Stephan, K.E., 2004. On the role of general system theory for functional neuroimaging. *J. Anat.* 205 (6), 443–470.
- Talairach, J., Tournoux, P., 1988. *Co-planar Stereotaxic Atlas of the Human Brain*. Thieme Medical Publishers, Inc., New York.
- Todd, J.J., Marois, R., 2004. Capacity limit of visual short-term memory in human posterior parietal cortex. *Nature* 428 (6984), 751–754.
- Vincent, J.L., Patel, G.H., Fox, M.D., Snyder, A.Z., Baker, J.T., Van Essen, D.C., Zempel, J.M., Snyder, L.H., Corbetta, M., Raichle, M.E., 2007. Intrinsic functional architecture in the anaesthetized monkey brain. *Nature* 447 (7140), 83–86.
- Visscher, K.M., F. Miezin, M., Kelly, J.E., Buckner, R.L., Donaldson, D.I., McAvoy, M.P., Bhalodia, V.M., Petersen, S.E., 2003. Mixed blocked/event-related designs separate transient and sustained activity in fMRI. *NeuroImage* 19 (4), 1694–1708.
- Wager, T.D., Barrett, L.F., 2004. From affect to control: functional specialization of the insula in motivation and regulation. Published online at PsycExtra.
- Wager, T.D., Smith, E.E., 2003. Neuroimaging studies of working memory: a meta-analysis. *Cogn. Affect. Behav. Neurosci.* 3 (4), 255–274.
- Wager, T.D., Jonides, J., Reading, S., 2004. Neuroimaging studies of shifting attention: a meta-analysis. *NeuroImage* 22 (4), 1679–1693.
- Wilk, M.B., Gnanadesikan, R., 1968. Probability plotting methods for the analysis of data. *Biometrika* 55 (1), 1–17.
- Xiong, J., Parsons, L.M., Gao, J.H., Fox, P.T., 1999. Interregional connectivity to primary motor cortex revealed using MRI resting state images. *Hum. Brain Mapp.* 8 (2–3), 151–156.